Turkish Journal of Electrical Engineering & Computer Sciences

http://journals.tubitak.gov.tr/elektrik/

Research Article

Turk J Elec Eng & Comp Sci
(2019) 27: 961 – 972

doi:10.3906/elk-1608-145

Design and development of a Stewart platform assisted and navigated transsphenoidal surgery

Selçuk KİZİR*, **Zafer BİNGÜL**
Department of Mechatronics Engineering, Faculty of Engineering, Kocaeli University, Kocaeli, Turkey

Received: 12.08.2018 • **Accepted/Published Online:** 10.12.2018 • **Final Version:** 22.03.2019

Abstract: In this study, technical details of a Stewart platform (SP) based robotic system as an endoscope positioner and holder for endoscopic transsphenoidal surgery are presented. Inverse and forward kinematics, full dynamics, and the Jacobian matrix of the robotic system are derived and simulated in MATLAB/Simulink. The required control structure for the trajectory and position control of the SP is developed and verified by several experiments. The robotic system can be navigated using a six degrees of freedom (DOF) joystick and a haptic device with force feedback. Position and trajectory control of the SP in the joint space is achieved using a new model-free intelligent PI (iPI) controller and it is compared with the classical PID (proportional-integral-derivative) controller. Trajectory tracking experimental results showed that the tracking performance of iPI is better than that of PID and the total RMSE of the trajectory tracking is decreased by 17.64% using the iPI controller. The validity of the robotic system is proven in the endoscopic transsphenoidal surgery performed on a realistic head model in the laboratory and on a cadaver in the Institute of Forensic Medicine. The key feature of the system developed here is to operate the endoscope via the joystick or haptic device with force feedback under iPI control. Usage of this system helps surgeons in long, fatiguing, and complex operations. This system can generate new possibilities for transsphenoidal surgery such as fully automated robotic surgery systems.

Key words: Endoscope holder, endoscope positioner, endoscopic transsphenoidal surgery, haptic device, intelligent PID, medical robotics, parallel manipulator, Stewart platform

1. Introduction

Robots have been started to be used in the field of medicine for solving problems as in every field and today many studies on this subject continue extensively. The purpose of medical robotics can be defined as providing new treatment options for surgeons rather than replacing surgeons with robots. Robots have been used to enhance and complement surgeons' capabilities or help surgeons in many medical areas [1].

Robots used in the medical applications can be serial, parallel, or hybrid structures. Parallel and serial robots have been frequently used in the medical field as well as in industry for the solution of many problems. Parallel robots are superior to serial robots in terms of basic robot features such as payload capacity, positioning accuracy, repeatability, and rigidity. Serial robots are superior in another important feature: large workspace and reachability. Recently, the best robotic solutions for surgery are obtained using hybrid robotic structures. The Stewart platform used widely in industry is a special parallel manipulator type. It allows six DOF precision motions like a surgeon's hand, which is important in robotic surgery. This structure is also known as hexapod and it was developed as a flight simulator and tire test machine by Stewart and Gough [2]. In the literature,

*Correspondence: selcuk.kizir@kocaeli.edu.tr

there are numerous reports and studies about medical robots and robotic surgery. Robotic systems have been used in branches such as orthopedics and traumatology; ear, nose, and throat; ophthalmology; gynecology; urology; plastic surgery; and brain and cardiovascular surgery [3]. Parallel robots focus on particular areas such as bone placement, fixing broken bones, spinal drilling and screw driving, knee replacement, hip replacement, skull drilling, and rehabilitation [3, 4].

Haptic devices have an important place in robotic surgery [5]. Haptic systems can be defined briefly as mechatronic devices that provide navigation with a variety of degrees of freedom and sense of touch using force feedback [6]. These structures can be designed based on the electromechanical or electromagnetic principles to be used in various workspaces. Haptic devices undertake the important task of ensuring the interaction between the surgeon and the robot in the field of robotic surgery, which gives the sense of touch, especially with the force feedback [7]. Another important application area of haptic systems is virtual training environments. Training of inexperienced surgeons brings significant costs, and also it improves the inefficient use of the operating rooms and their equipment. Interns are trained with plastic models, live animals, and humans. An intern has the possibility of making more errors in comparison with a specialist surgeon and these errors can have economic, legal, and social effects. For these reasons, surgical simulators are known to be educational options, because they provide a cost-effective and efficient methodology. Medical simulators have been developed inspired by aircraft simulators. Surgical virtual reality simulators offer better education and exercises without endangering the lives of patients. Candidate surgeons can do exercises for different challenging scenarios. In addition, it eliminates the need for the use of live animals or cadavers.

Surgical procedures are used very intensively with images obtained by a microchip camera as an endoscope with the developments in imaging and optical systems. This can be called endoscopic or laparoscopic surgery and robots have been used in this area for the solutions of problems as well. Endoscopic transsphenoidal surgery [8], a minimal invasive procedure, aims to remove tumors within the sphenoid sinus and sella turcica of the skull. This procedure is one of the medical fields that needs robotic assistance. In the literature, there are several commercial robotic systems and research studies related to robotic assistance. Ballester et al. [9] compared the task performance of laparoscopic camera holders Endo Assist and AESOP (Automated Endoscopic System for Optimal Positioning) and stated that Endo Assist was quicker than AESOP in the downward, sideways, and diagonal tasks. AESOP was only faster in preprogrammed complex tasks and no difference for zoom motions was seen between them. Nathan et al. [10] used the AESOP system in order to approach the sella. Nimsky et al. [11] adopted the Evolution 1 robot attached with a 6 DOF hexapod used as an instrument holder operated by a joystick for extended endoscope assisted transsphenoidal surgery. Bumm et al. [12] developed a serial robot based robotic system for endoscopic transsphenoidal surgery. Burgner et al. [13] and Chalongwongse and Suthakorn [14] studied workspace requirements for robot assisted endonasal transsphenoidal surgery and designed a concentric tube continuum robot [13] and a hybrid 6 DOF robot in which a delta parallel robot was proposed for 3 DOF translation and 2 DOF for rotation and 1 DOF for surgical tool insertion. The required workspace was determined by an optical tracking system and computed tomography (CT) images.

This study presents the results of the development of a haptic and joystick navigated Stewart platform for endoscope positioning and holding in transsphenoidal surgery. The aim of the study is to examine the feasibility of usage of a haptic or joystick navigated Stewart platform in transsphenoidal surgery. A new model-free intelligent PI controller was also used for the first time for position and trajectory control of the SP. The rest of the paper is organized as follows: In Section 2, components of the robotic surgery system are described. In Section 3, kinematics and dynamics of the SP, controller design, stability, and experimental studies on a skull

model and cadavers for endoscopic transsphenoidal surgery are given. Finally, conclusions are presented and future work is recommended.

2. Materials and methods

Figure 1 depicts the block diagram of the overall system, which consists of the SP and other parts such as real-time controller (ds1103), 6-DOF joystick (space navigator), 6-DOF haptic device (Phantom Omni), 6-DOF force-torque sensor (Ati-Gamma), controller-robot connector board, emergency stop circuit, power supply, and endoscope holder. The surgeons are able to select one of the navigation devices (joystick or haptic) to operate the robot. The reference trajectory is then produced by the selected navigation device. The endoscope position is controlled according to the surgeon's instructions.

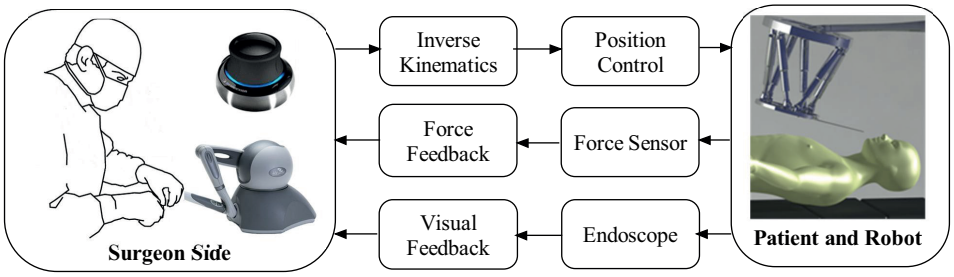

Figure 1. General structure of the robotic surgery system.

The SP system has a special structure that includes two main bodies (upper mobile and bottom fixed plates), six linear actuators, and universal joints. Implementation of control algorithms was realized using the DSPACE DS1103 real-time controller.

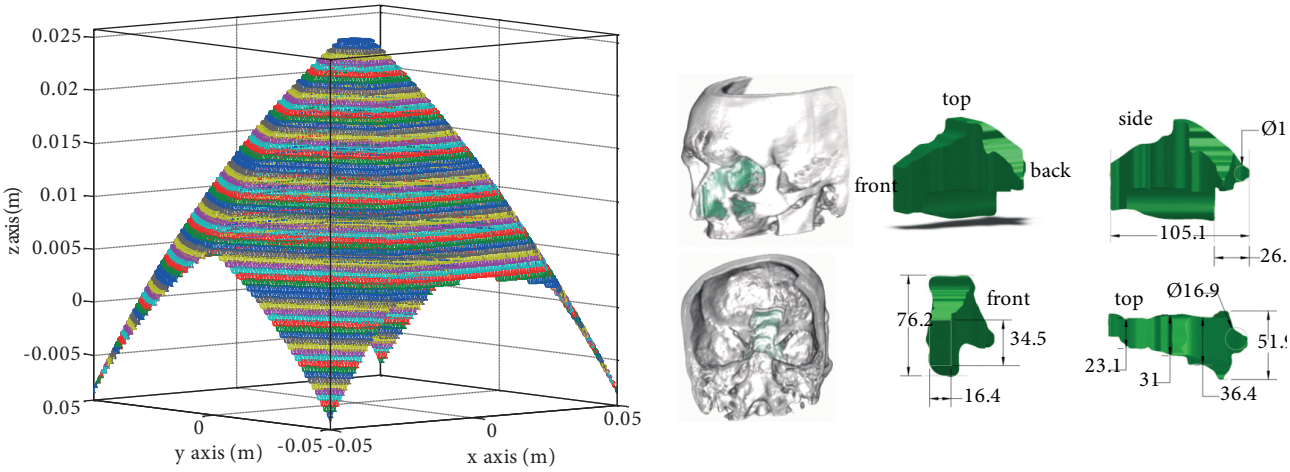

Figure 2. (a)Workspace of the SP used in this study. (b) Maximum surgical workspace for average sized endonasal skull base surgery (mm) [13].

The maximum workspace for the operation of endonasal skull base surgery was found to be a cylindrical space with 24.2 mm for diameter and 100.6 mm for length in [14] and 100 mm distance from the nostril entrance to the pituitary in [13], respectively. The calculated workspace of the SP under zero orientation is shown in Figure 2a. The maximum space required for the endonasal surgery calculated by [13] is shown in Figure 2b.

The robot's workspace is sufficient for the operation, but a new kinematic design can be developed in the case of the need for a larger workspace. The Phantom Omni haptic device was developed by the Sensable Company. It is capable of six degrees of freedom position sensing, providing three degrees of freedom force feedback. Haptic devices are used in many applications, such as virtual reality, robot navigation, and telerobotics. The Phantom Omni can be programmed using the OpenHaptics library with C++. In order to be integrated into the system and navigate the SP with the haptic device, a VisualStudio 2008 project was developed in the C++ environment. Reflection of the force was provided by the force/torque sensor at the base of the endoscope holder. An Ati gamma sensor was used to sense three axis forces and 19,200 bps serial communication speed was used between the ds1103 controller and haptic device. In communication, 3 bytes of data were used for the force feedback and 6 bytes of data were used and sent for the orientation and position commands. The robot could be navigated with a joystick instead of the 6 DOF haptic device. A 3D mouse (space navigator, 3Dconnexion) enabled the production of three-dimensional motions. An m-file was written in MATLAB for reading the joystick via USB. Motion commands yielded by users were transmitted to the ds1103 controller board via the RS-232 serial port.

3. Results

3.1. Kinematics and dynamics of the SP

Robot kinematics defines the geometric relationships between Cartesian and joint space of a robot. Coordinate systems can be placed at the center of the upper mobile plate and base plate in order to find the inverse kinematics of the SP as depicted in Figure 3. Bi (i = 1, 2, .. 6) and Ti (i = 1, 2, .. 6) coordinate systems show the connection points of each leg.

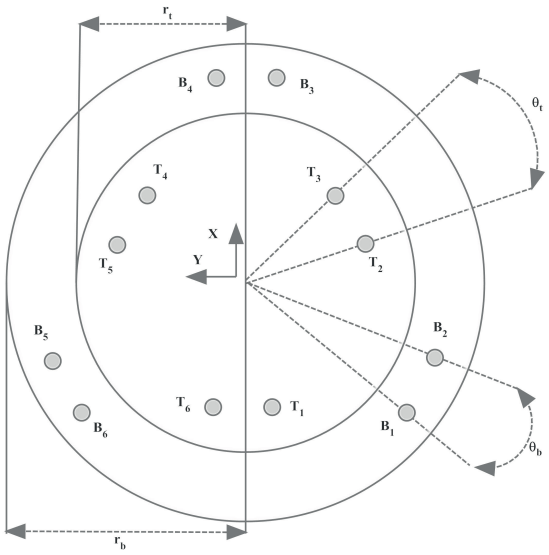

Figure 3. Kinematic configuration of the SP.

These connection points can be computed from

$$\boldsymbol{T_i} = \begin{bmatrix} T_{ix} \\ T_{iy} \\ T_{iz} \end{bmatrix} = \begin{bmatrix} r_t \cos(\lambda_i) \\ r_t \sin(\lambda_i) \\ 0 \end{bmatrix} \quad \boldsymbol{B_i} = \begin{bmatrix} B_{ix} \\ B_{iy} \\ B_{iz} \end{bmatrix} = \begin{bmatrix} r_b \cos(\nu_i) \\ r_b \sin(\nu_i) \\ 0 \end{bmatrix}. \tag{1}$$

$$\lambda_i = \frac{i\pi}{3} - \frac{\theta_t}{2} \qquad i = 1,\ 3,\ 5 \quad and \quad \lambda_i = \lambda_{i-1} + \theta_t \qquad i = 2,\ 4,\ 6. \tag{2}$$

$$\nu_i = \frac{i\pi}{3} - \frac{\theta_b}{2} \qquad i = 1,\ 3,\ 5 \quad and \quad \nu_i = \nu_{i-1} + \theta_b \qquad i = 2,\ 4,\ 6. \tag{3}$$

θ_b and θ_t are the angles between coordinates, and r_b and r_t are the radii of the bottom and top plates, respectively. The leg vectors can be computed from the following equation: [15],

$$\boldsymbol{L_i = R_{XYZ} T_i + P - B_i} \quad i = 1,\ 2,\ ..., 6. \tag{4}$$

$\boldsymbol{P}$ is the position vector and $\boldsymbol{R}$ is the orientation matrix. Finally, leg lengths are the norms of the vectors. Forward kinematics can be defined by calculation of the robot tool point from the known joint values. In this study, online and offline forward kinematics of the SP were solved by the Newton–Raphson numerical iteration method based on the inverse kinematics solution. Accordingly, the equation needing to be solved is shown below:

$$f(i) = (R_{11}T_{ix} + R_{12}T_{iy} + p_x - B_{ix})^2 + (R_{21}T_{ix} + R_{22}T_{iy} + p_y - B_{iy})^2 + (R_{31}T_{ix} + R_{32}T_{iy} + p_z)^2 - (l(i) + l_{nominal})^2. \tag{5}$$

This nonlinear equation can be solved by using the Newton–Raphson algorithm, whose equations are given below:

$$\Gamma_{ij} = \frac{\partial f_i}{\partial x_j}, \tag{6}$$

$$x^{(\upsilon+1)} = x^{(\upsilon)} - \Gamma^{-1(\upsilon)} f^{\upsilon}. \tag{7}$$

In order to find the relevant Γ_{ij}, first, the row of the Γ matrix can be obtained based on partial derivatives. Finally, an embedded MATLAB function was written in Simulink for this algorithm. The Jacobian matrix is another important topic and can be defined as follows:

$$\boldsymbol{\dot{L} = J\dot{X}}, \tag{8}$$

$$\boldsymbol{\tau = J^T F}. \tag{9}$$

$\boldsymbol{J}$, $\boldsymbol{\dot{L}}$, $\boldsymbol{X}$, $\boldsymbol{\tau}$, and $\boldsymbol{F}$ represent the Jacobian matrix, leg velocity vector, end effector velocities, joint torques, and force applied to the actuators, respectively.

The forward dynamics of the SP is expressed by the following equation in Cartesian space [16]:

$$\boldsymbol{M(X)\ddot{X} + C\left(X, \dot{X}\right)\dot{X} + G(X) = \tau}. \tag{10}$$

$\boldsymbol{M}$ stands for the 6×6 symmetric and positive definite mass matrix, $\boldsymbol{C}$ for the Coriolis and centripetal matrix, $\boldsymbol{G}$ for the gravity vector, $\boldsymbol{\tau}$ for the applied torque vector, and $\boldsymbol{X}$ for the position and orientation of the upper plate. The full model of the system with addition of actuator dynamics can be obtained as below:

$$L_a \frac{di_a}{dt} + R_a i_a = V_a - K_b \dot{\theta}, \tag{11}$$

$$\tau_m - \tau_l = J_m\ddot{\theta} + B_m\dot{\theta}. \tag{12}$$

L_a is the inductance (H), i_a is the current (A), R_a is the resistance (Ω), V_a is the applied voltage (V), K_b is the back EMF constant (V/rpm), θ is the motor position (rad), τ_m is motor the torque (Nm), τ_l is the load torque, J_m is the total inertia (kgm^2), and B_m is the total damping (Nms/rad). The matrix form of Eq. (12) can be defined as follows:

$$\boldsymbol{\tau_m = M_a\ddot{L} + N_a\dot{L} + K_aY}. \tag{13}$$

$\boldsymbol{M_a} = \frac{2\pi}{p}(J_m)\boldsymbol{I_{6x6}}$, $\boldsymbol{N_a} = \frac{2\pi}{p}(B_m)\boldsymbol{I_{6x6}}$, $\boldsymbol{K_a} = \frac{p}{2\pi}\boldsymbol{I_{6x6}}$, $Y = \frac{2\pi}{p}\tau_l$, and p is the ball screw pitch. Finally, the full dynamics of the SP is achieved by [17]:

$$\boldsymbol{\tau_m = \check{M}_f\ddot{X} + \check{N}_f\dot{X} + \check{G}_f}, \tag{14}$$

$$\boldsymbol{\check{M}_f = M_aJ + K_aJ^{-T}M}, \quad \boldsymbol{\check{N}_f = N_aJ + M_a\dot{J} + K_aJ^{-T}C}, \quad \boldsymbol{\check{G}_f = K_aJ^{-T}G}. \tag{15}$$

Figure 4 shows a block diagram of Eq. (14), which represents the full dynamic model of the SP and a Simulink model designed for simulations about position and trajectory control of the SP.

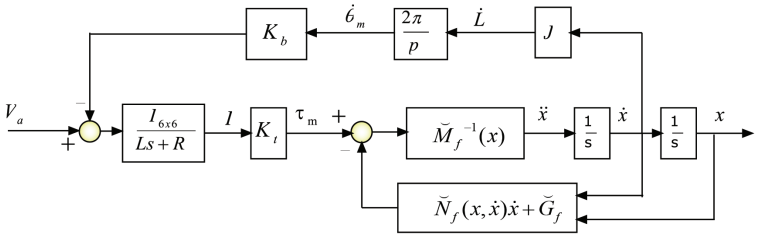

Figure 4. Full dynamic model diagram of the SP.

3.2. Position control

The SP position controller can be designed in the Cartesian space or joint space. Forward kinematics is required for position control of the SP in the Cartesian space, whereas the design of the controller in the joint space needs inverse kinematics. Forward kinematics is a difficult problem; however, inverse kinematics is an easier task to solve for parallel manipulators. Therefore, the position controller of the SP was designed in joint space. Position control in Cartesian space was transformed into leg position control in the joint space. A novel intelligent PI (iPI) control method [18–20] was used for the position and trajectory control of the SP. Intelligent PID controllers show better control performance than classic PID controllers, as demonstrated in [18–20]. This is achieved because intelligent PID controllers can be tuned in a quite straightforward and natural way in contrast to the classical PID [20]. An iPID controller is similar to a classical PII^{2}D controller [20]. A new model-free intelligent PI controller [18] is defined for n = 1:

$$\dot{y} = F + \beta u, \tag{16}$$

$$u = \frac{F - \dot{y^*}}{\beta} + K_pe + K_i\int e, \tag{17}$$

where $e = y^* - y$ is the error, y^* is the reference trajectory, K_p and K_i are the proportional and integrator tuning gains, and β is a constant parameter. For the implementation, Eqs. (16) and (17) were slightly modified [19]:

$$\dot{y}(t) = \tilde{F}(t) + \beta u(t-\lambda), \tag{18}$$

$$u = \frac{\tilde{F}(t) - \dot{y^*}(t)}{\beta} + K_p(y^*(t) - y(t)) + K_i \int (y^*(t) - y(t))dt, \tag{19}$$

where $\tilde{F}(t)$ is the current estimate of $F(t)$ calculated by Eq. (20) with the first derivative of the current output measurement ($\dot{y}(t)$) and previous input ($u(t-\lambda)$):

$$\tilde{F}(t) = \dot{y}(t) - \beta u(t-\lambda). \tag{20}$$

Stability analysis of the iPI controller can be found in [19] and it was shown that if β and controller parameters are selected such that the $s^2 + \beta K_p s + \beta K_i$ polynomial is Hurwitz then three cases are obtained:

Case I: If either $\lambda \to 0$ or $\mid z \mid << \frac{1}{\sqrt{\beta\lambda}}$, then model-free control is achieved and the controller gains can be selected using the Routh–Hurwitz stability criterion.

Case II: If $\beta\lambda \mid z \mid^2 \to \infty$, then three closed-loop poles are located at the origin of the s-plane, which is unstable.

Case III: A parameter-based tuning of the system is required, where Case I must be provided to make the system stable, and if so, dominant poles are located at:

$$s_{1,2} = \frac{(-\beta K_p \mp \sqrt{\beta^2 K_p^2 - 4\beta K_i})}{2}. \tag{21}$$

Under these conditions the iPI controller was designed and compared with the classical PID. Under the same conditions, 4 different point to point smooth trajectory (Kane functions) tracking experiments were conducted in the z axis for 2 s. Results of the experiments are given in the Table (best performance shown in bold) with controller parameters of total error costs (RMSE), controller effort, and RMSE error costs of each leg. The performance index used in the table is the root mean squared error (RMSE) defined as $RMSE = \sqrt{\frac{1}{N}\sum_{i=1}^{N}(e(t)^2)}$. Results showed that an improvement of 15.68% was achieved from Exp. IV compared to I, an improvement of 10.78% from Exp. IV to II, and an improvement of 17.64% from Exp. IV to III according to the total cost values. This comparison shows that any of the iPIs has better tracking performance than the classical PID in the trajectory experiments.

One of the real-time experimental position responses under haptic navigation is given in Figure 5. In the figure, reference orientation and position commands applied by the haptic device and robot position in Cartesian space computed from joint space values using forward kinematics are shown. The response of the actuators or joint space according to the motion in Figure 5 is shown in Figure 6, which proves Figure 5. The three axis forces exerted during the experiment, which are also reflected by the haptic device, are shown in Figure 7. The haptic device used in this study allows three axis force feedback, which provides tactile feedback to the surgeon. Force feedback is especially important in robotic surgery, but it is not crucial for endoscope

Table. Comparison of trajectory tracking performances for the iPI and classical PID.

Exp.	Parameters	Total cost	Control effort	Leg1	Leg2	Leg3	Leg4	Leg5	Leg6
1	β:2 F: 0.1 Kp:10 Ki:20	0.0086	0.2722	0.0020	**0.0013**	0.0014	0.0013	0.0014	0.0013
2	β:2 F: 0.02 Kp:10 Ki:20	0.0091	0.2723	0.0021	0.0015	0.0015	0.0014	0.0015	0.0012
3	β:0.4 F: 0.02 Kp:10 Ki:20	**0.0084**	0.2822	0.0019	0.0014	**0.0014**	**0.0012**	**0.0013**	**0.0012**
4	Kp:10 Ki:20 Kd:0.006	0.0102	0.2799	**0.0017**	0.0017	0.0016	0.0023	0.0015	0.0013

positioning, especially in transsphenoidal surgery. The surgeon can be feel the tool/tissue interaction by the haptic device with tactile feedback, for example when the endoscope touches the body. Gaining touch sense for the surgeon is an important capability in robotic surgery.

3.3. Endoscopic transsphenoidal surgery

Endoscopic transsphenoidal surgery is a special surgical operation in neurosurgery [8, 21]. It aims at evacuation of the tumor in the pituitary gland. High-resolution endoscopes are used in this surgery for viewing. The operation is carried out through the patient's nostrils. In order to access it through the sphenoid sinus, the nasal cavity must be prepared first. Figure 8 is a view of the endoscopic approach to the pituitary gland region. Furthermore, the nasal cavity, sphenoid sinus, and tuberculum sella, which is almost inaccessible today by endoscopic tools, can be seen in the figure [13]. After the patient is prepared for the surgery, the surgeon has to hold and direct the endoscope using one hand during surgery. Surgeons try to operate and use surgical equipment under video guides with the other hand. The surgeons may be tired during a long operation. Therefore, surgeons may perform the surgery alternately, so there are more surgeons than necessary at the same time. This is also critical, because two or more operations may be carried out if the hospital has qualified facilities. To eliminate these disadvantages, a high precision parallel manipulator can be used as an endoscope positioner. For this reason, a SP based robotic system is developed, which can be navigated by a six DOF haptic device and joystick. The workspace of the haptic device and the SP was matched to each other. The joystick was designed to work incrementally and the haptic device may also be designed to work incrementally. The surgeons should use the haptic device when continuous trajectory tracking and force feedback are required. Also, the haptic device allows mapping surgeons' hand movements with endoscope motion. Surgeons should use the joystick when fundamental commands such as stop or move in any direction are needed. The Cartesian position and orientation commands produced by the haptic device were converted to leg lengths using the inverse kinematics. Force signals produced by the 6 DOF force/torque sensor were processed and reflected by the haptic device at the same time. A series of experimental tests were conducted on a realistic skull model

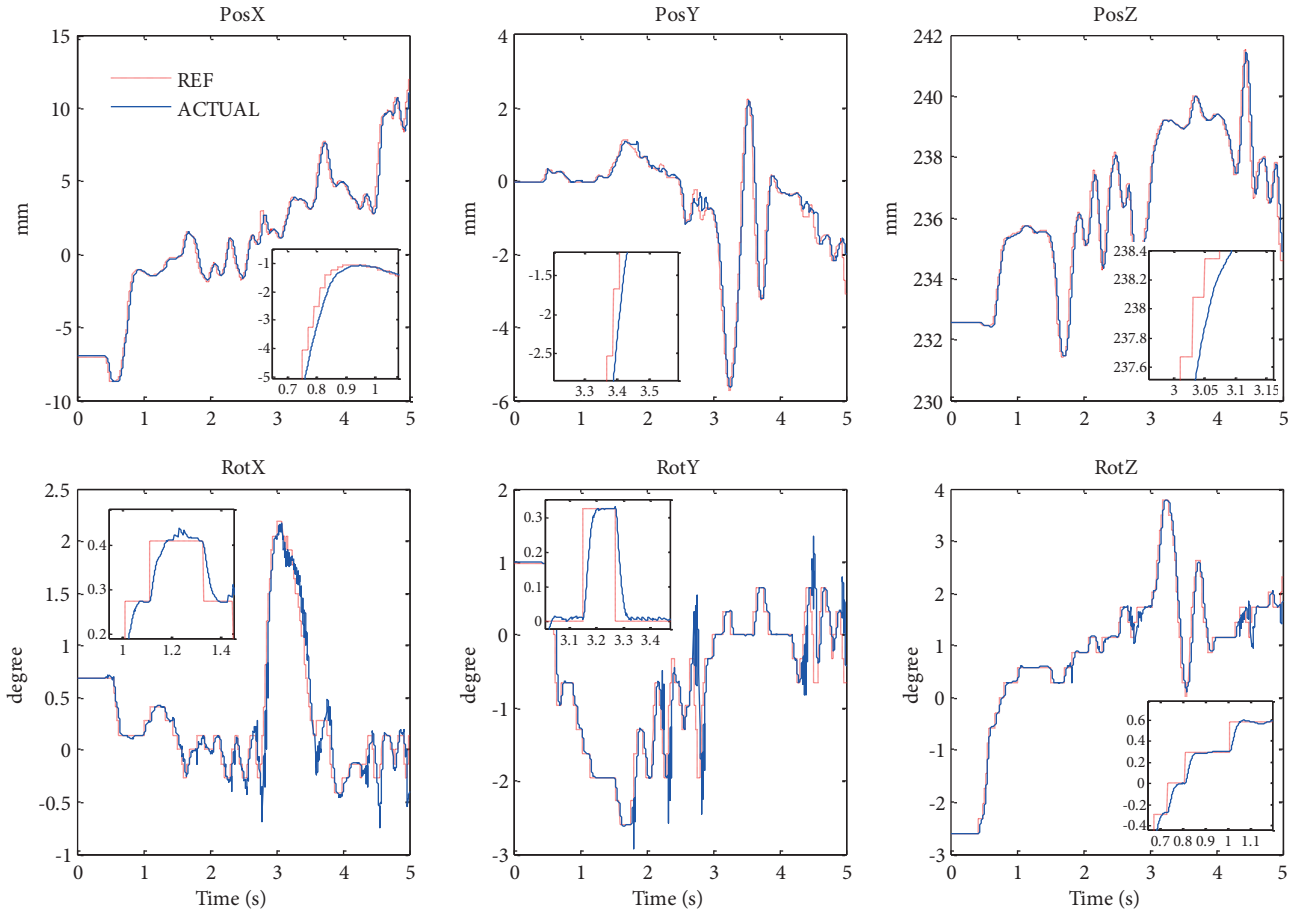

Figure 5. Trajectory control of the SP with haptic device in Cartesian space.

in the laboratory. A photograph of the experimental setup is shown in Figure 9a. After laboratory tests on the model, some experiments were carried out on cadavers with neurosurgeons in order to demonstrate the effectiveness of the system. The demonstration on a fresh cadaver is shown in Figure 9b. Comments about the usage of this system in endoscopic transsphenoidal surgery from the medical point of view can be found in [22].

4. Conclusion

The SP allows high resolution manipulation so it can be used in robotic surgery with high precision motions. In this study, a SP based robotic system was developed for an endoscope positioner and holder especially in endoscopic transsphenoidal surgery. In this surgery, the endoscope can be navigated by the SP in the full operation space with six DOF joystick and haptic device. The haptic device allows three axis force feedback, which is important in robotic surgery, but it is not crucial for endoscope positioning. Some criticisms may be mentioned about the system: robot placement and size of the upper plate. Some suggestions about robot placement can be given in order to use the developed system more effectively. The robot can be connected to the ceiling of the operating room using a device like a surgery lamp or a serial manipulator. As a future study, a wheeled station can be designed to hold the SP or adapted to a serial manipulator. On the other hand, the workspace of the surgeon can be restricted by the upper plate. In order to overcome this drawback,

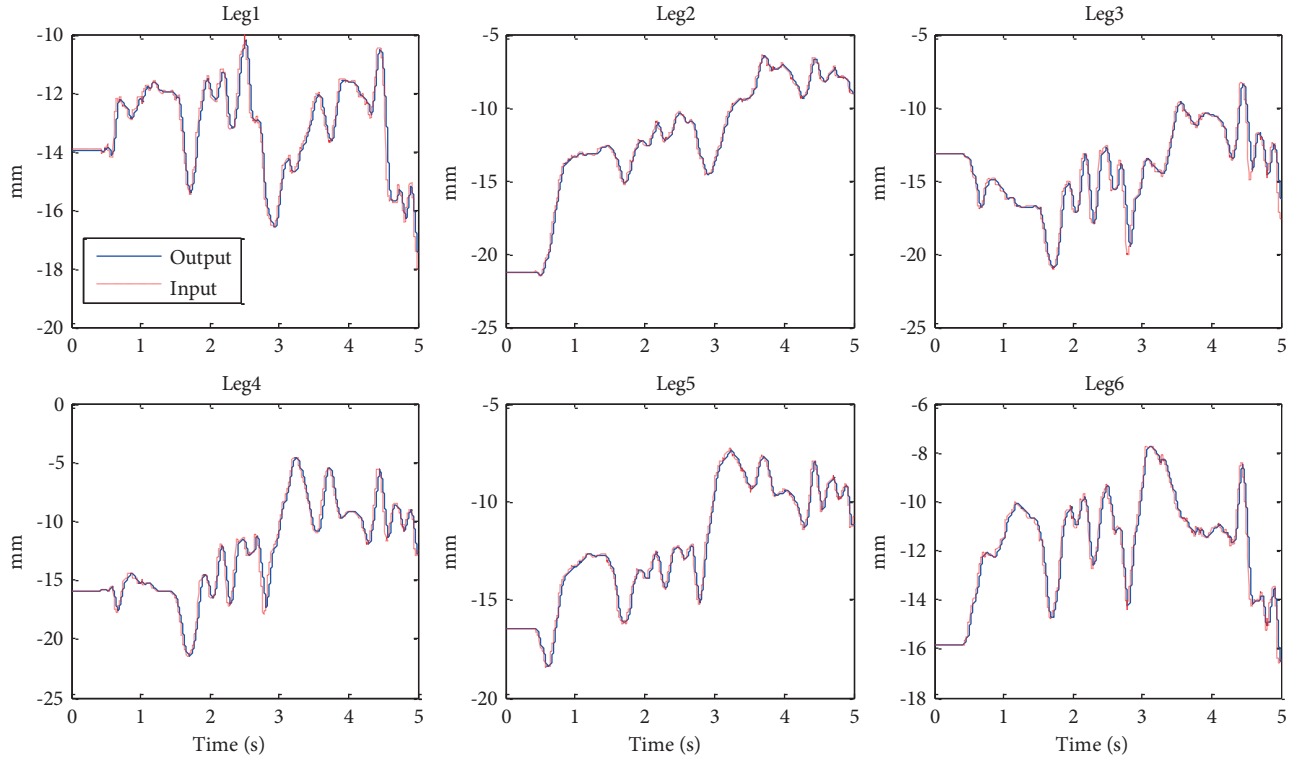

Figure 6. Trajectory control of the SP with haptic device in joint space.

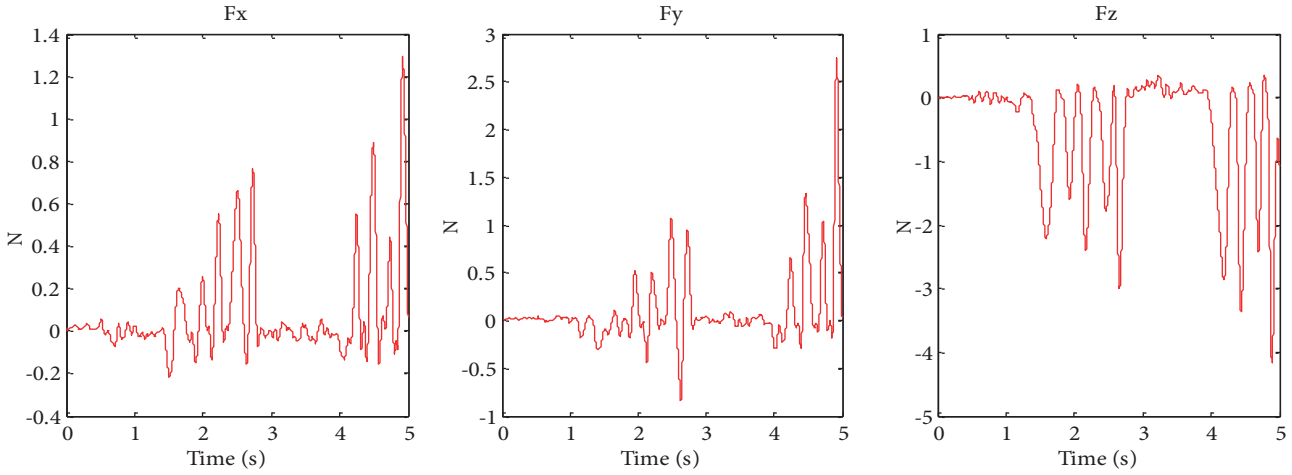

Figure 7. Three axis forces reflected by haptic device during above motion.

a new kinematic design of the SP can be studied (smaller, lighter, etc.) or the robot can hold and navigate an instrument holder with the endoscope simultaneously. Furthermore, a prismatic axis can be attached to the top platform in order to increase the workspace. In summary, the SP based robotic system developed here is feasible for transsphenoidal surgery and results can lead to new possibilities in the area of transsphenoidal surgery such as fully automated robotic surgery systems with integration of the navigation system.

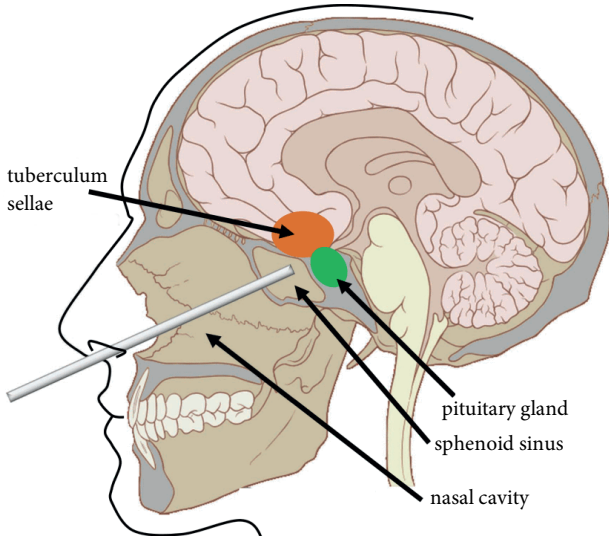

Figure 8. Pituitary gland region in the brain [13].

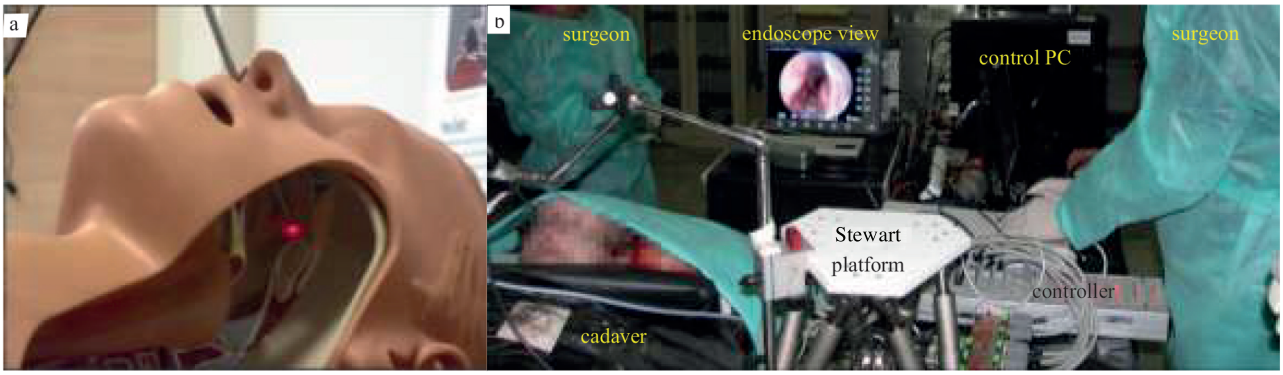

Figure 9. (a) An experiment performed on realistic skull model. (b) An experiment performed on a fresh cadaver.

Acknowledgments

The authors are deeply grateful to the Department of Neurosurgery at the Kocaeli University School of Medicine and Institute of Forensic Medicine for providing medical guidance, and especially Prof Dr Savaş Ceylan's constructive advice on the current subject. The authors would like to thank the Scientific and Technological Research Council of Turkey (TÜBİTAK) for the SP used in this study under Grant No. 107M148.

References

[1] Gourin CG, Terris DJ. Robotics in Surgery: History, Current and Future Applications. 1st ed. New York, NY, USA: Nova Science Publishers, 2007.

[2] Merlet JP. Parallel Robots. 2nd ed. Berlin, Germany: Springer, 2006.

[3] Bozovic V. Medical Robotics. 1st ed. Graz, Austria: I-Tech Education and Publishing, 2008.

[4] Barkana DE. Design and implementation of a control architecture for a robot-assisted orthopedic surgery. International Journal of Medical Robotics and Computer Assisted Surgery 2010; 6: 42-56.

[5] Díaz I, Gil JJ, Louredo M. A haptic pedal for surgery assistance. Computer Methods and Programs in Biomedicine 2014; 116: 97-104.

[6] Hayward V, Astley OR, Cruz-Hernandez M, Grant D, Robles-De La Torre G. Haptic interfaces and devices. Sensor Review 2004; 24: 16-29.

[7] Tavakoli M, Patel RV, Moallem M. Haptic interaction in robot-assisted endoscopic surgery: a sensorized end-effector. International Journal of Medical Robotics and Computer Assisted Surgery 2005; 1: 53-63.

[8] Ceylan S, Koç K, Anık İ. Endoscopic endonasal transsphenoidal approach for pituitary adenomas invading the cavernous sinus. J Neurosurg 2010; 112: 99-107.

[9] Ballester P, Jain Y, Haylett KR, McCloy RF. Comparison of task performance of robotic camera holders EndoAssist and Aesop. International Congress Series 2001; 1230: 1100-1103.

[10] Nathan CO, Chakradeo V, Malhotra K, D'Agostino H, Patwardhan R. The voice-controlled robotic assist scope holder AESOP for the endoscopic approach to the sella. Skull Base: An Interdisciplinary Approach 2006; 16: 123-131.

[11] Nimsky C, Rachinger J, Iro H, Fahlbusch R. Adaptation of a hexapod-based robotic system for extended endoscope-assisted transsphenoidal skull base surgery. Minimally Invasive Neurosurgery 2004; 47: 41-46.

[12] Bumm K, Wurm J, Rachinger J, Dannenmann T, Bohr C, Fahlbuch R, Iro H, Nimsky C. An automated robotic approach with redundant navigation for minimal invasive extended transsphenoidal skull base surgery. Minimally Invasive Neurosurgery 2005; 48: 159-164.

[13] Burgner J, Rucker DC, Gilbert HB. A telerobotic system for transnasal surgery. IEEE/ASME Transactions on Mechatronics 2013; 19(3): 996-1006.

[14] Chalongwongse S, Suthakorn J. Workspace determination and robot design of a prototyped surgical robotic system based on a cadaveric study in endonasal transsphenoidal surgery. In: 2014 IEEE International Conference on Robotics and Biomimetics (ROBIO 2014); 2014; Bali. pp. 241-246.

[15] Huang C, Chang C, Yu M, Fu L. Sliding-mode tracking control of the Stewart platform. In: 5th Asian Control Conference; 20–23 July 2004; Melbourne, Australia. pp. 562-569.

[16] Lin J, Chen CW. Computer-aided-symbolic dynamic modeling for Stewart-platform manipulator. Robotica 2009; 27: 331–341.

[17] Kizir S, Bingül Z. Fuzzy impedance and force control of a stewart platform. Turkish Journal of Electrical Engineering and Computer Sciences 2014; 22: 924-939.

[18] Fliess M, Join C. Model-free control and intelligent PID controllers: towards a possible trivialization of nonlinear control? In: 15th IFAC Symposium on System Identification; 6–8 July 2009; Saint-Malo, France. pp. 1-62.

[19] Agee JT, Kizir S, Bingul Z. Intelligent proportional-integral (iPI) control of a single link flexible joint manipulator. Journal of Vibration and Control 2015; 21: 2273-2288.

[20] d'Andréa-Novel B, Fliess M, Join C, Mounier H, Steux B. A mathematical explanation via "intelligent" PID controllers of the strange ubiquity of PIDs. In: 18th Mediterranean Conference on Control Automatation; 2010; Marrakesh, Morocco.

[21] Jho HD. Endoscopic transsphenoidal surgery. Journal of Neuro-oncology 2001; 54: 187-195.

[22] Cabuk B, Ceylan S, Anik I, Tugasaygi M, Kizir S. A haptic guided robotic system for endoscope positioning and holding. Turkish Neurosurgery 2015; 25: 601-607.